

# Application of Nomarski Differential Interference Contrast Microscopy to Highlight the Prior Austenite Grain Boundaries Revealed by Thermal Etching

D. San Martín<sup>1\*</sup>, Y. Palizdar<sup>2</sup>, R.C. Cochrane<sup>2</sup>, R. Brydson<sup>2</sup> and A.J. Scott<sup>2</sup>

<sup>1</sup>MATERIALIA Group, Centro Nacional de Investigaciones Metalúrgicas (CENIM-CSIC), Department of Physical Metallurgy, Av. Gregorio del Amo 8, 28040 Madrid, Spain

<sup>2</sup>Institute for Materials Research, SPEME, University of Leeds, Leeds LS2 9JT, UK.

\*Corresponding Author:

David San Martín.

Centro Nacional de Investigaciones Metalúrgicas (CENIM-CSIC).

Department Physical Metallurgy.

Avda Gregorio de Amo 8, 28040.

Madrid, Spain.

Email: [dsm@cenim.csic.es](mailto:dsm@cenim.csic.es)

Tel: 0034 915538900.

Fax: 0034 915347425.

**Abstract:**

Revealing prior austenite grain boundaries by thermal etching has been demonstrated to be a reliable and fast method compared to chemical etching for microalloyed carbon steels. However, sometimes visualisation of the thermally etched prior austenite grain boundaries is hindered by the presence of grain boundaries of other phases (e.g. ferrite and/or pearlite) which are thermally etched during slow cooling from high temperature. This work shows that, under these conditions, the use of Nomarski Differential Interference Contrast microscopy under bright field illumination helps to highlight the thermally etched prior austenite grain boundaries.

**Keywords:** Low-carbon steel; Austenite; Grain boundary; Thermal etching; Optical microscopy; Nomarski microscopy.

## 1. Introduction.

Determining the prior austenite grain size in steels remains **is extremely important** for metallurgists due to its key influence on the transformations taking place during cooling and, thus, on the final properties. With new steels coming to the market every year, reliable procedures to reveal the prior austenite grain boundaries in a wide range of steel compositions are needed.

The thermal etching method has been demonstrated **to be** a reliable and fast method **for** revealing the **prior austenite grain boundaries** in carbon microalloyed steels [1,2], but, technically, this technique can be applied to any other alloy. It only requires the preparation of a finely polished surface of the **specimen** (1  $\mu\text{m}$  diamond cloth) and the application of high vacuum conditions during the heat treatment to avoid oxide formation that would darken the polished surface. At high temperatures, preferential diffusion takes places at the intersection of the austenite grain boundaries and the free polished surface, forming grooves of **approximately 1-2  $\mu\text{m}$**  in width (Fig. 1 [3]). After heating, slow cooling is generally preferred to fast cooling because the latter promotes the formation of surface reliefs due **to martensitic** and/or bainitic transformations. **However, in certain cases**, the phases formed during cooling (ferrite, pearlite, precipitates) can hinder/mask the **prior austenite grain boundaries** formed at high temperature as it will be shown in this work. This study shows that using Nomarski differential interference contrast microscopy (**from now on referred to as Nomarski microscopy**) under bright field illumination helps to **reveal the prior austenite grain boundaries** compared to other phase boundaries. Nomarski microscopy, invented by G. Nomarski in the mid-1950s [4,5,6], has been commonly used to image **specimens** which contain poor optical contrast when viewed using **bright field** illumination. Using Nomarski **microscopy**, microtopographic differences on the surface of the **specimen** are thrown into sharp

relief, permitting better resolution of micro-textures. Examples can be found in the scientific literature where Nomarski microscopy has been applied in addition to bright field reflection illumination [7,8] but, to the authors' knowledge, no paper has described the use of this technique in highlighting thermally etched prior austenite grain boundaries of microstructures lacking good contrast under bright field illumination. As a demonstration, a low carbon steel has been investigated in this work.

## 2. Materials and Procedures.

The chemical composition of the steel under investigation is given in Table 1. Experimental details regarding the processing of the steel and the initial microstructure can be found elsewhere [9,10]. Machined cylindrical dilatometric specimens of 10 mm in length and 4 mm in diameter were used for this investigation. In order to reveal the prior austenite grain boundaries by thermal etching, these specimens were first mounted in bakelite and, then, a surface of 2-3 mm in width was polished parallel to the main axis of the cylinder using standard metallographic techniques, finishing with 1  $\mu\text{m}$  diamond cloth. The specimens were then carefully removed from the bakelite to avoid damaging the polished surface. The heat treatments were carried out in a Bahr 805D high resolution dilatometer under high vacuum conditions ( $10^{-5}$  mbar) to prevent oxide formation on the polished surface. The specimens were heated following a multi-step cycle: 1) heating rate of 14  $^{\circ}\text{C}/\text{s}$  up to 650  $^{\circ}\text{C}$ ; 2) heating rate of 6.6  $^{\circ}\text{C}/\text{s}$  up to 900  $^{\circ}\text{C}$ ; and 3) heating rate of 2  $^{\circ}\text{C}/\text{s}$  up to the final austenitization temperature above the  $A_{c3}$  temperature (for this steel,  $A_{c3}\sim 904\pm 1$   $^{\circ}\text{C}$ ) and held for 600 s. After the austenitization heat treatment, specimens were cooled to room temperature at an average cooling rate of 5  $^{\circ}\text{C}/\text{s}$ . Two different austenitization temperatures have been investigated, 1000 and 1150  $^{\circ}\text{C}$ , with the aim of obtaining significantly

different **prior austenite grain sizes**. The metallographic inspection of the as-heat treated **specimens** was carried out with an optical microscope Nikon Epiphot 200 using Nomarski **microscopy** under **bright field** reflection illumination.

### **3. Results and Discussion.**

Figure 2 **shows images** obtained for **specimens** heat treated at 1000 °C for 600 s. At low magnification, the **bright field** image in Figure 2a) shows a network of grain **boundaries which**, except for a few grains, it is difficult to **differentiate those corresponding to prior austenite grain boundaries** or to ferrite grain boundaries, these latter phase boundaries also being thermally etched during cooling. Using Nomarski **microscopy** (Figure 2b)), the **prior austenite grain boundaries are** clearly differentiated from **ferrite grain boundaries** and the **prior austenite grain size** can be easily determined by image analysis. Analysis of more than 200 **grains revealed** an average austenite grain size (feret diameter) of 42 µm. Figures 2c)-d) **show** higher magnification images of the microstructures obtained after heating at 1000 °C for 600 s. At this magnification **the majority** of the **prior austenite grain boundaries**, although weakly revealed, can **just be distinguished using bright field** illumination (Figure 2c)). **However, after using bright field illumination** combined with Normaski microscopy (Figure 2d)) the **prior austenite grain boundaries** are **now** clearly outlined and the **prior austenite grain size** can be measured more accurately.

Figures 3 shows the results obtained after heating at 1150 °C for 600 s. At low magnification (Figure 3a) thermal etching gives much better contrast when, as here, the **prior austenite grain size** is sufficiently **large** and the network of **ferrite grain boundaries does** not significantly mask the prior austenitic microstructure. The results **obtained** under **bright field** illumination may be

acceptable in estimating the [prior austenite grain size](#). However, Figure 3b again shows that the use of Normarski [microscopy](#) highlights the [prior austenite grain boundaries](#) more clearly. After the analysis of more than 200 grains, the average feret diameter determined for this microstructure by image analysis was 185  $\mu\text{m}$ .

In addition to highlighting [prior austenite grain boundaries](#), Figure 4 demonstrates the ability of Normarski [microscopy](#) to reveal other features present in the microstructure such as twins, [ferrite grain boundaries](#) or ghost [prior austenite grain boundaries](#). The [prior austenite grain boundaries indicated by the](#) arrows in Figure 4b have been weakly revealed by thermal etching but are perfectly visible using Normarski microscopy. Ghost boundaries (Figure 4b and 4f) are relics of [prior austenite grain boundaries](#) thermally etched at an early stage of the heat treatment at high temperatures and not completely filled by diffusion of iron atoms on the surface after the boundary has moved forward to another location. These ghost [prior austenite grain boundaries](#) could be removed from the surface if rapid cooling from the austenite phase field is applied instead of slow cooling, with the aim of forming martensite and/or bainite [2]. However, the formation of surface [reliefs](#), promoted by these transformations on the polished surface, would not only mask the ghost [prior austenite grain boundaries](#), but also diminish the effective visualization of the thermally etched [prior austenite grain boundaries](#); this problem would be more pronounced for smaller grain sizes ( $<30 \mu\text{m}$ ).

In addition, Figure 4f shows that the positions of ghost [prior austenite grain boundaries](#) compared to the actual [prior austenite grain boundaries](#) generated just before cooling, helps to show the direction of movement of the [prior austenite grain boundaries](#) (direction of the dashed arrows) during austenite grain growth.

From these results, it is evident that the use of the thermal etching method for revealing the **prior austenite grain boundaries** examined in an optical microscope using Nomarski **microscopy** under **bright field** illumination is extremely useful in outlining many features of the prior austenitic microstructure in cases where **bright field** illumination might be insufficient. Moreover, light chemical etching of the thermally etched polished surface with, for example, Nital-2% would show directly, on the same **specimen**, the ferritic microstructure transformed on cooling and, thus, how the ferrite grains have grown from the prior austenitic microstructure. This would allow the investigation of the relationship between the prior austenite grain size and the ferritic grain structure, as well as how twins within austenite grains affect the growth of ferrite. When undertaking these suggested studies one should **note** that transformations taking place during cooling (**such as** the allotriomorphic ferrite transformation in the steel investigated) could **have a** slightly different **mechanism** on a free surface compared to the bulk.

#### **4. Conclusions.**

**It has been** demonstrated that the use of Nomarski differential interference contrast microscopy under bright field illumination significantly improves the observation **of prior** austenite grain boundaries revealed by using thermal etching methods compared to the use of **bright field** illumination alone. Furthermore, the approach described in this work enables the direct understanding of the relationship between the prior austenite microstructure at high temperatures and the microstructure (phases) **obtained after** cooling **to room temperature**.

## 5. Acknowledgements.

The authors would like to thank the Ministerio de Ciencia e Innovación (Proyecto Petri PET2007\_0326\_02) for funding this work. Javier Vara Miñambres and Nacho Ruiz Oliva from CENIM-CSIC are gratefully acknowledged for their experimental support with the dilatometry experiments and metallographic [specimen](#) preparation.

## 6. References.

- [1] C. García de Andrés, M.J. Bartolomé, C. Capdevila, D. San Martín, F.G. Caballero, V. López, Metallographic techniques for the determination of the austenite grain size in medium-carbon microalloyed steels, *Mater. Char.* 46 (2001) 389-398.
- [2] C. García de Andrés, F.G. Caballero, C. Capdevila, D. San Martín, Revealing austenite grain boundaries by thermal etching: advantages and disadvantages, *Mater. Char.* 49 (2003) 121-127.
- [3] Y. Amouyal, E. Rabkin, A scanning force microscopy study of grain boundary energy in copper subjected to equal channel angular pressing, *Acta Mater.* 55 (2007) 6681-6689.
- [4] Nomarski G, Weill AR. Sur l'observation des figures de croissance des cristaux par les methods interférentielles à deux ondes, 77. Société française de Minéralogie et de Cristallographie Bulletin; 77 (1954) 840-68.
- [5] R.D. Allen, G.B. David, and G. Nomarski, The Zeiss-Nomarski differential interference equipment for transmitted-light microscopy. *Z. Wiss. Mikrosk.* 69 (1969) 193-221.
- [6] J.F. Burke, G. Indebetouw, G. Nomarski, and G.W. Stroke, White-light three dimensional microscopy using multiple-image storing and decoding, *Nature* 231 (1971) 303-306.



- [7] F. Lefevre-Schlick, O. Bouaziz, Y. Brechet, J.D. Embury, Compositionally graded steels: The effect of partial decarburization on the mechanical properties of spherodite and pearlite, *Mater. Sci. Eng. A*, 491 (2008) 80-87.
- [8] J. Götze, Application of Nomarski DIC and cathodoluminescence (CL) microscopy to building materials, *Mater. Char.* 60 (2009) 594-602.
- [9] Y. Palizdar, R.C. Cochrane, R. Brydson, D. Crowther, D. San Martin, A.J. Scott, The effect of deliberate aluminium additions on the microstructure of rolled steel plate characterized using EBSD, *Mater. Char.* 61 (2010) 159-167.
- [10] Y. Palizdar, A. J. Scott, R. C. Cochrane and R. Brydson, Understanding the effect of aluminium on microstructure in low level nitrogen steels, *Mater. Sci. Tech.* 25 (2009) 1243-1248.

## Figure Captions.

Figure 1 Atomic Force Microscopy image of a groove formed by thermal etching in copper. Color image taken from Figure 3 in reference [3] which has been converted to a grayscale image.

Figure 2 Prior austenite grain boundaries revealed by thermal etching after heating to 1000 °C for 600 s and cooled at a rate of 5 °C/s; a), c) are bright field optical images, while b), d) are the same images after using Nomarski microscopy. The symbol  $T_\gamma$  refers to the austenitization temperature.

Figure 3 Prior austenite grain boundaries revealed by thermal etching after heating to 1150 °C for 600 s and cooled at a rate of 5 °C/s; a) is a bright field optical image, while b) is the same image after using Nomarski microscopy. The symbol  $T_\gamma$  refers to the austenitization temperature.

Figure 4 Microstructures revealed by thermal etching after heating to 1000 °C (a-b) and 1150 °C (c-f) for 600 s and cooled at a rate of 5 °C/s; a), c), e) are bright field optical images, while b), d) and f) are the same images, respectively, after using Nomarski microscopy. The acronym PAGB means Prior Austenite Grain Boundary and FGB means Ferrite Grain Boundary. The symbol  $T_\gamma$  refers to the austenitization temperature.

**Tables**

Table 1 Chemical composition of the steel investigated (wt.-%) with Fe to balance.

C	Mn	Si	P	S	Al	N
0.028	1.41	0.28	0.001	0.001	0.02	0.0022

Figure 1a

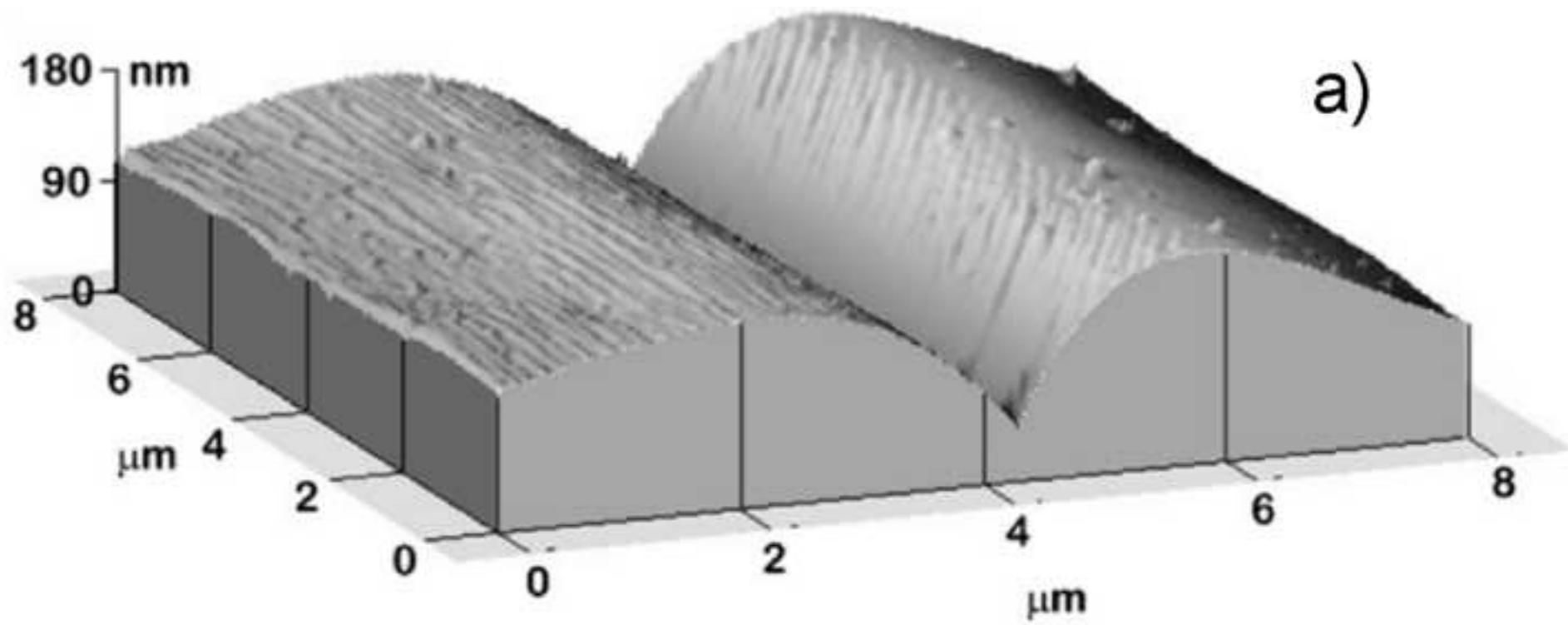


Figure 1b

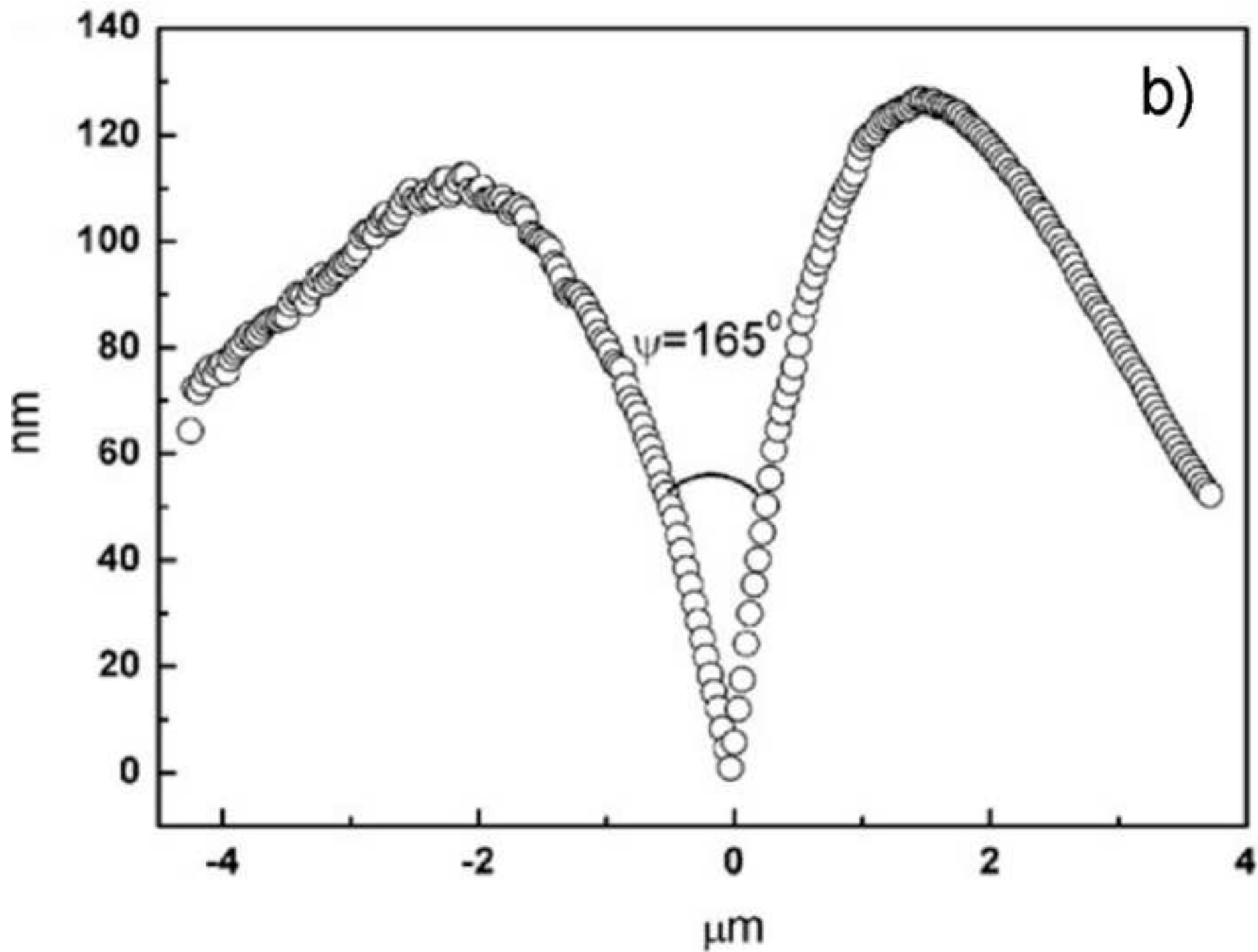


Figure 2a

**a)**  $T_{\gamma}=1000\text{ }^{\circ}\text{C}$ ; Bright field illumination

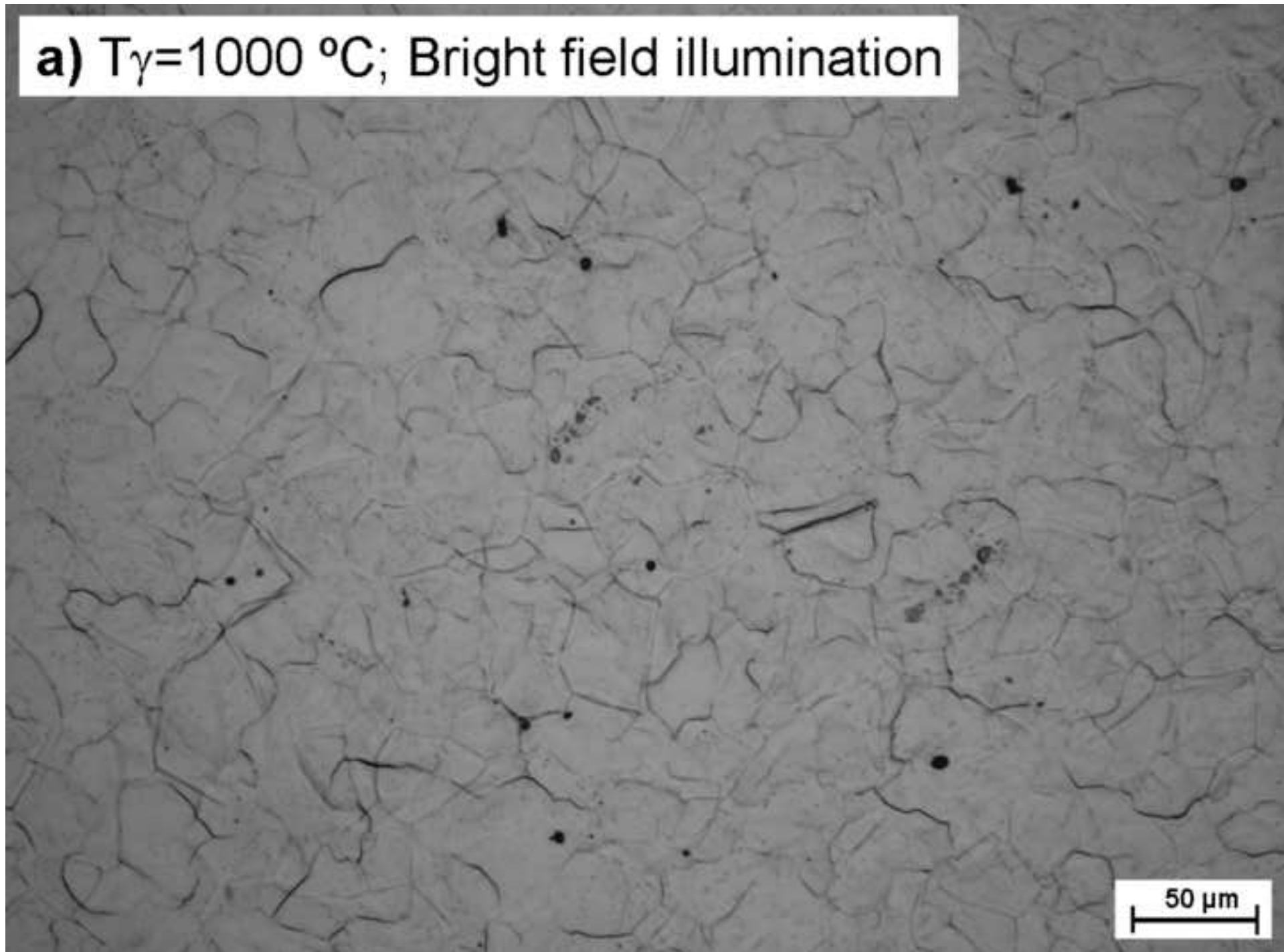


Figure 2b

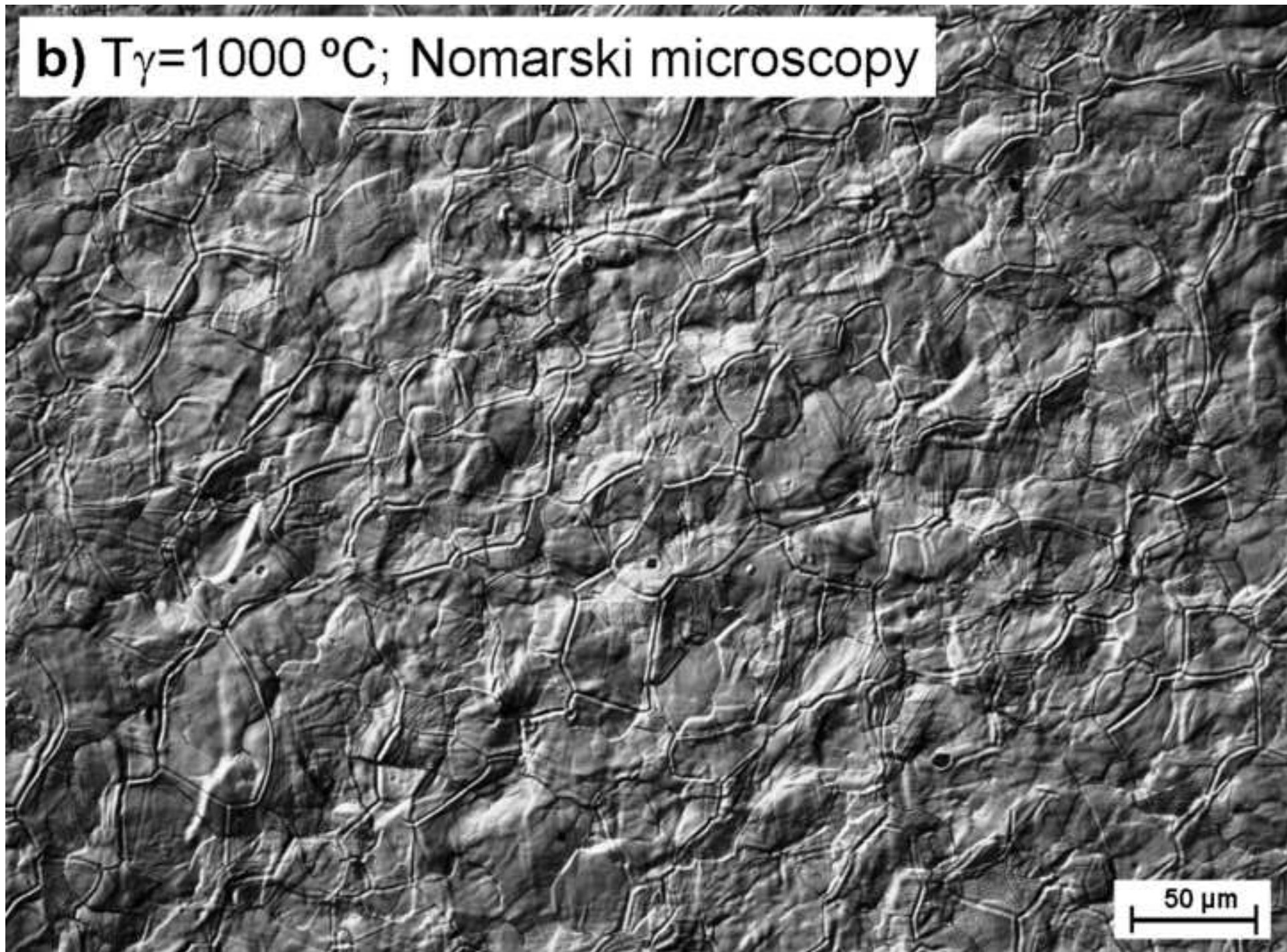


Figure 2c

**c)**  $T_{\gamma}=1000\text{ }^{\circ}\text{C}$ ; Bright field illumination

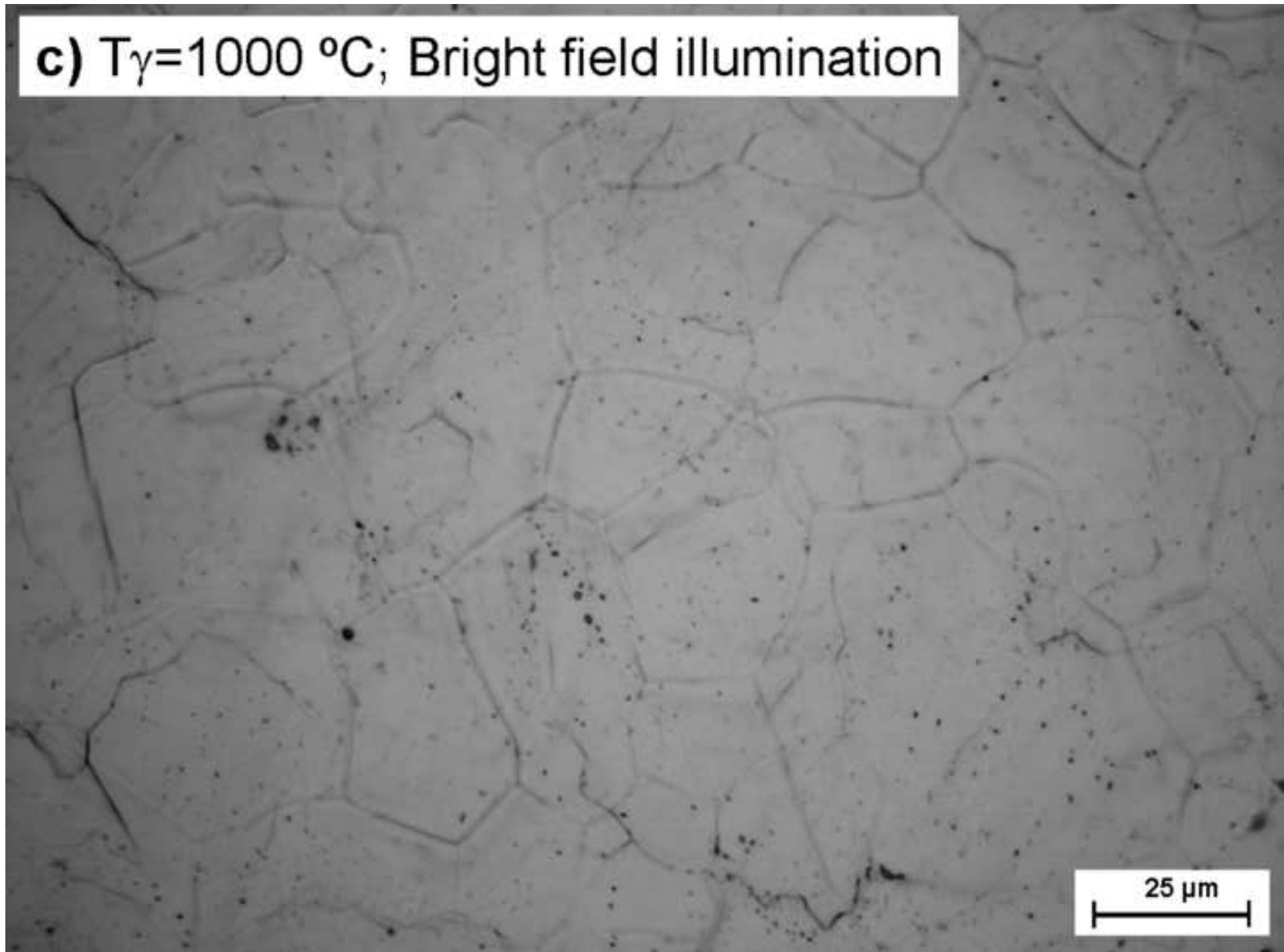




Figure 2d

**d)**  $T_{\gamma}=1000\text{ }^{\circ}\text{C}$ ; Nomarski microscopy

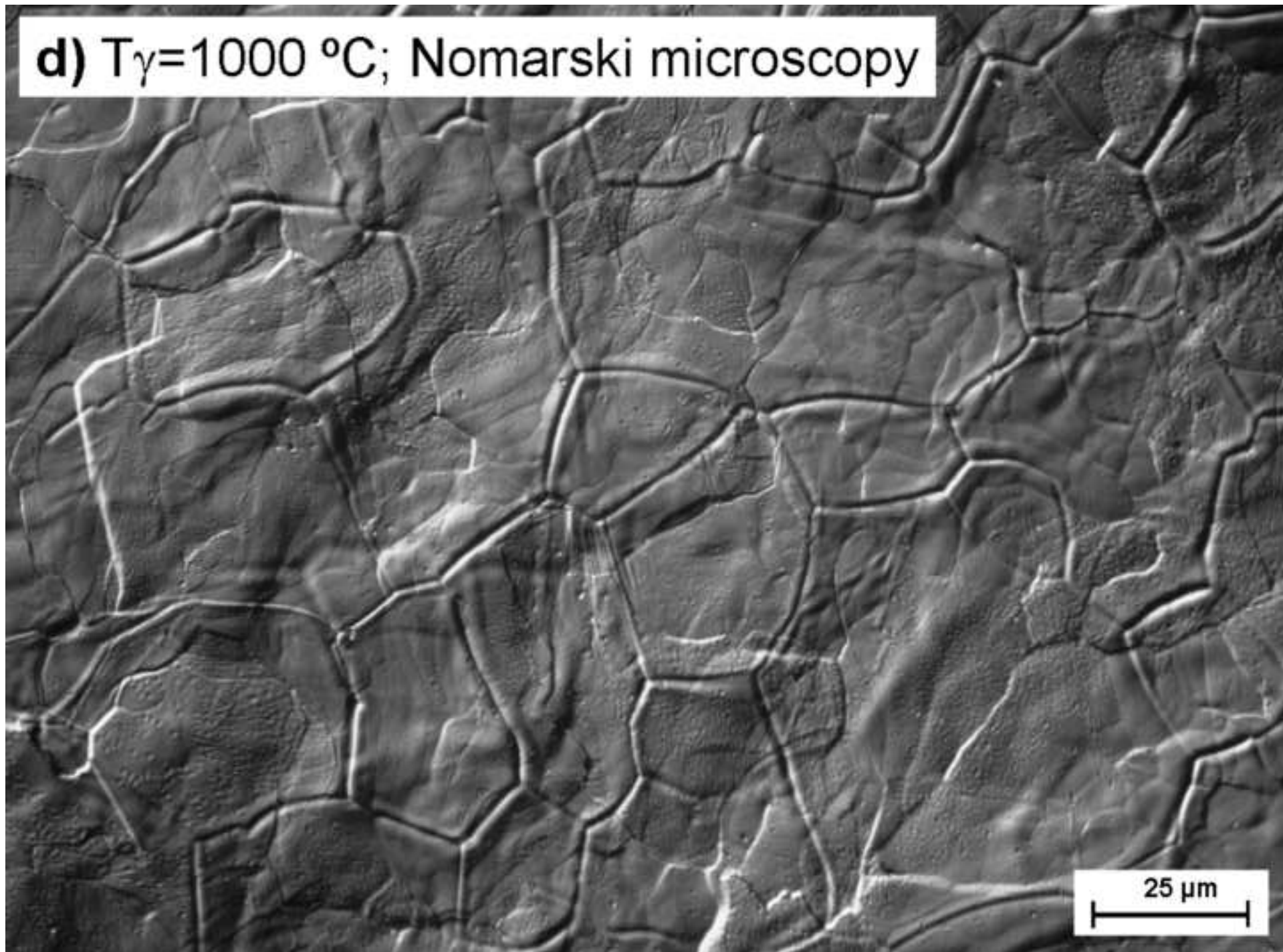


Figure 3a

**a)**  $T_{\gamma}=1150\text{ }^{\circ}\text{C}$ ; Bright field illumination

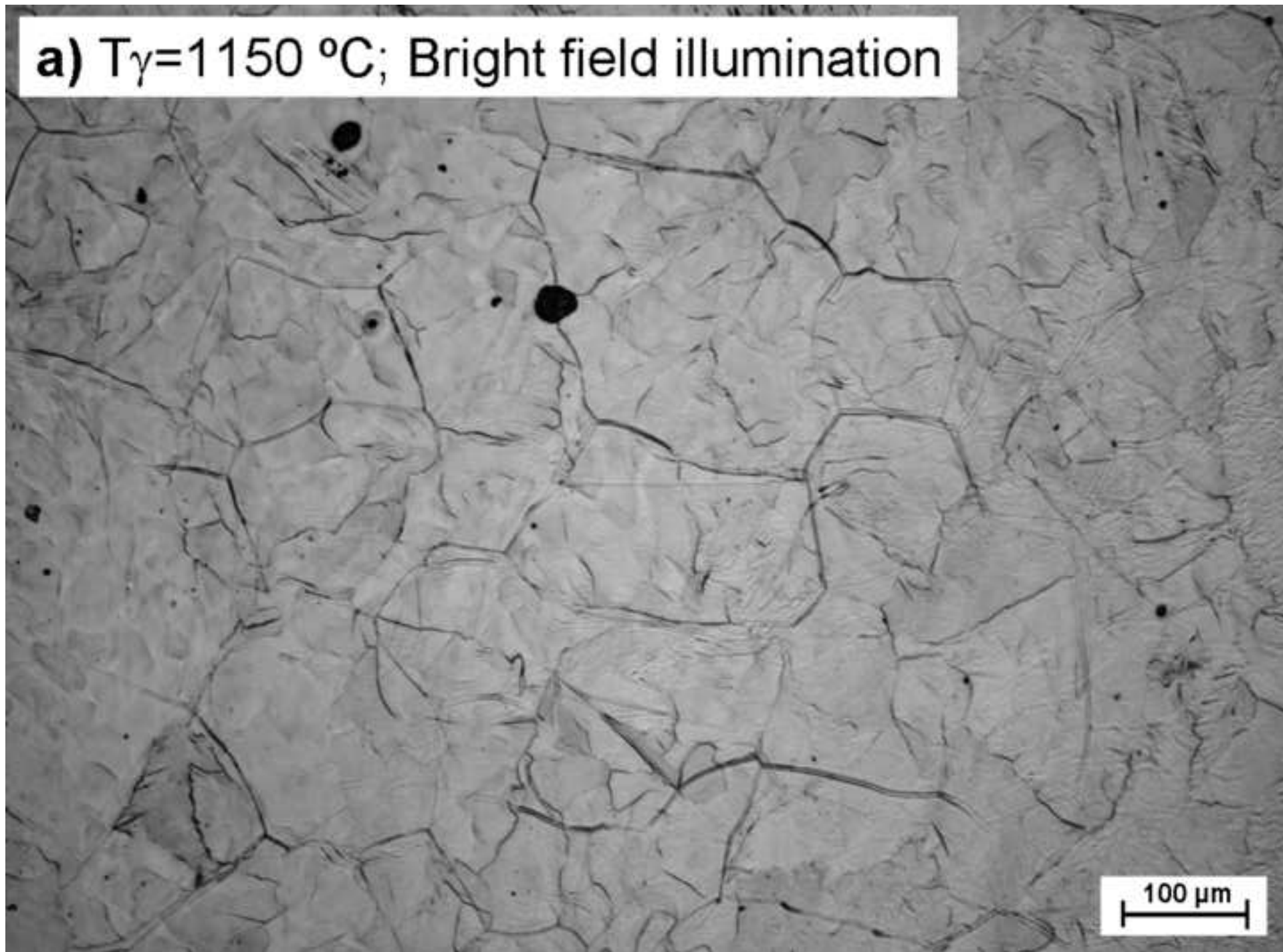
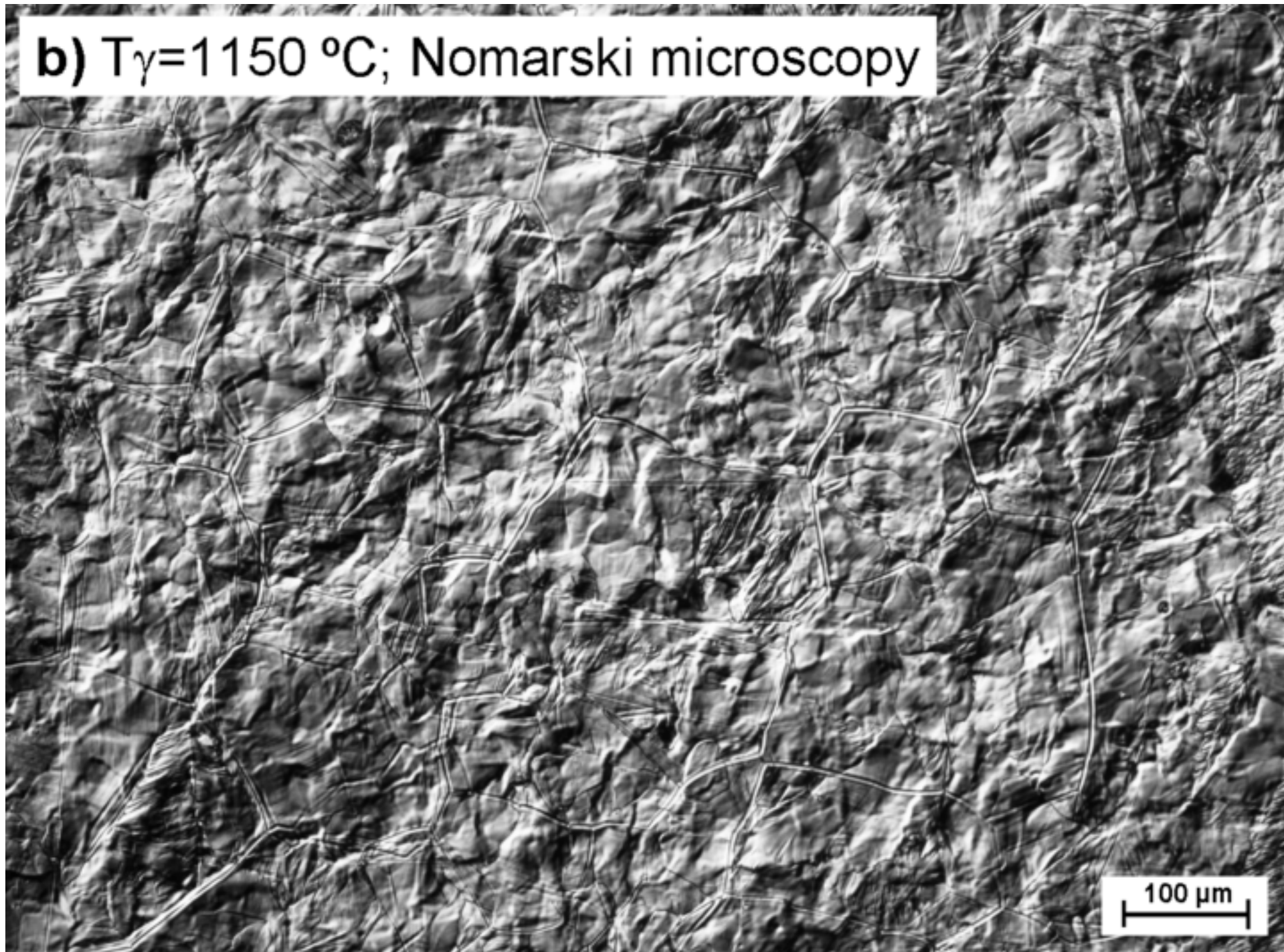


Figure 3b

**b)**  $T_{\gamma}=1150$  °C; Nomarski microscopy



**a)**  $T_{\gamma}=1000\text{ }^{\circ}\text{C}$ ; Bright field illumination

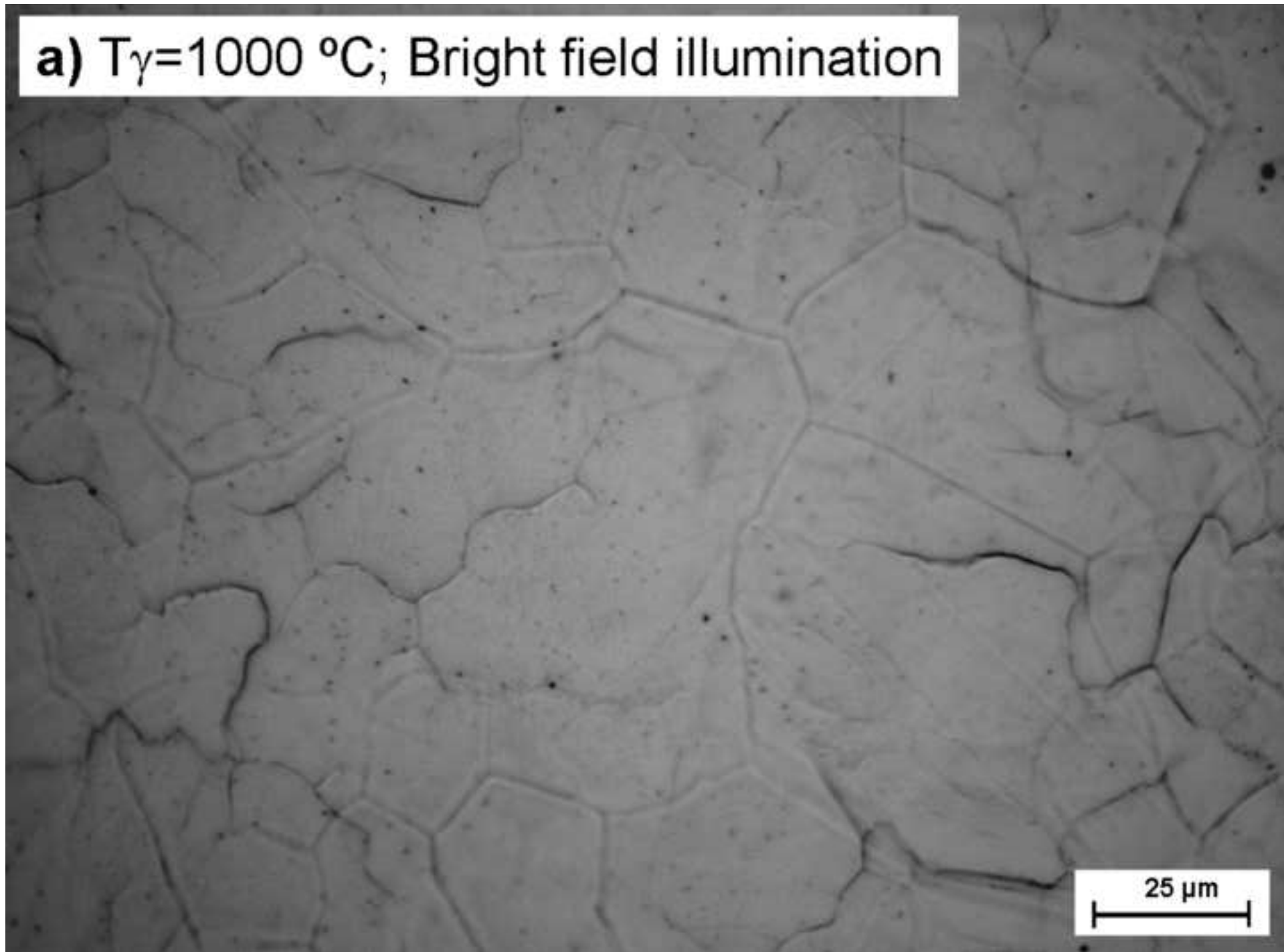
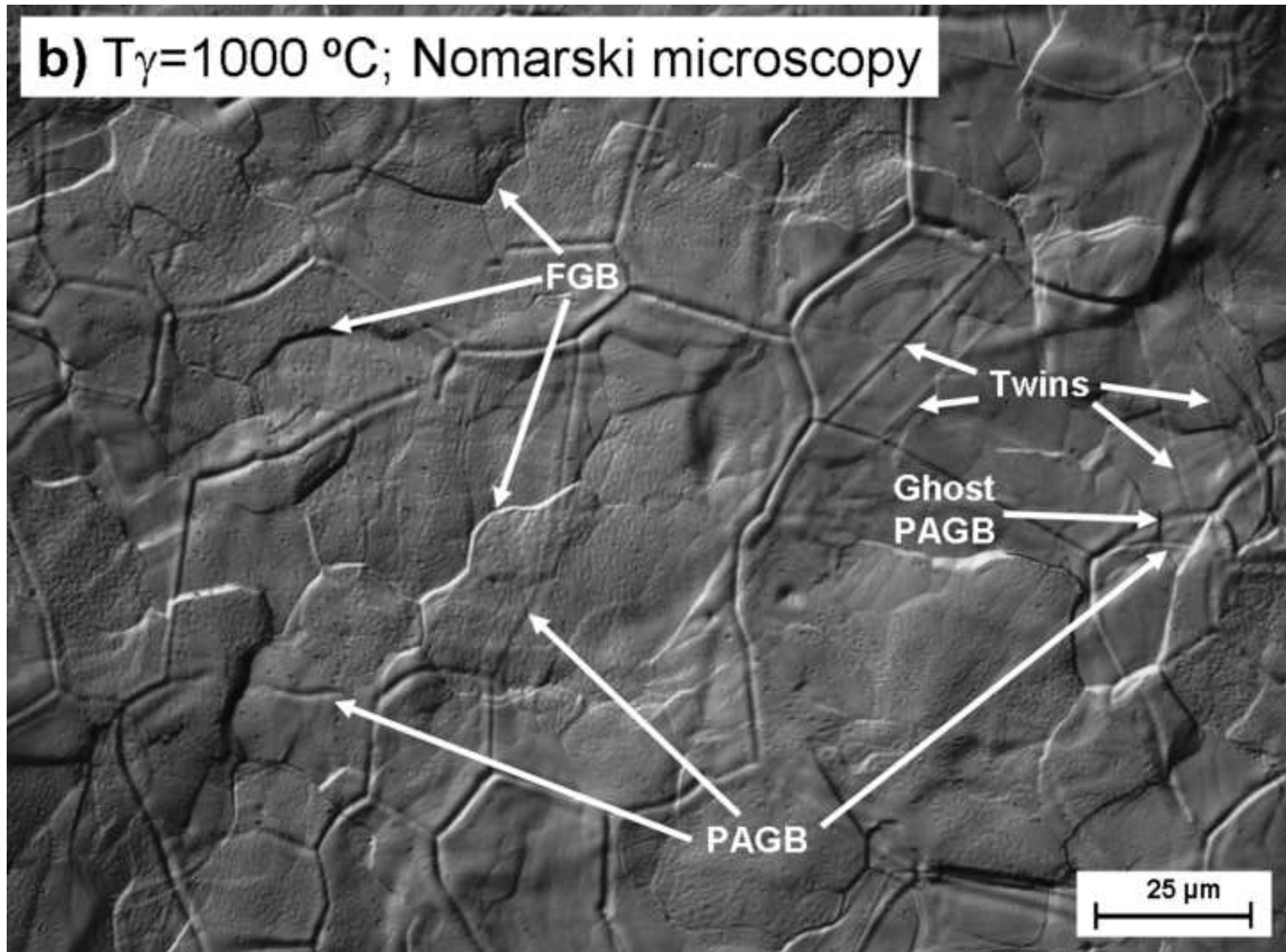


Figure 4b

**b)**  $T_{\gamma}=1000\text{ }^{\circ}\text{C}$ ; Nomarski microscopy



**c)**  $T_{\gamma}=1150$  °C; Bright field illumination

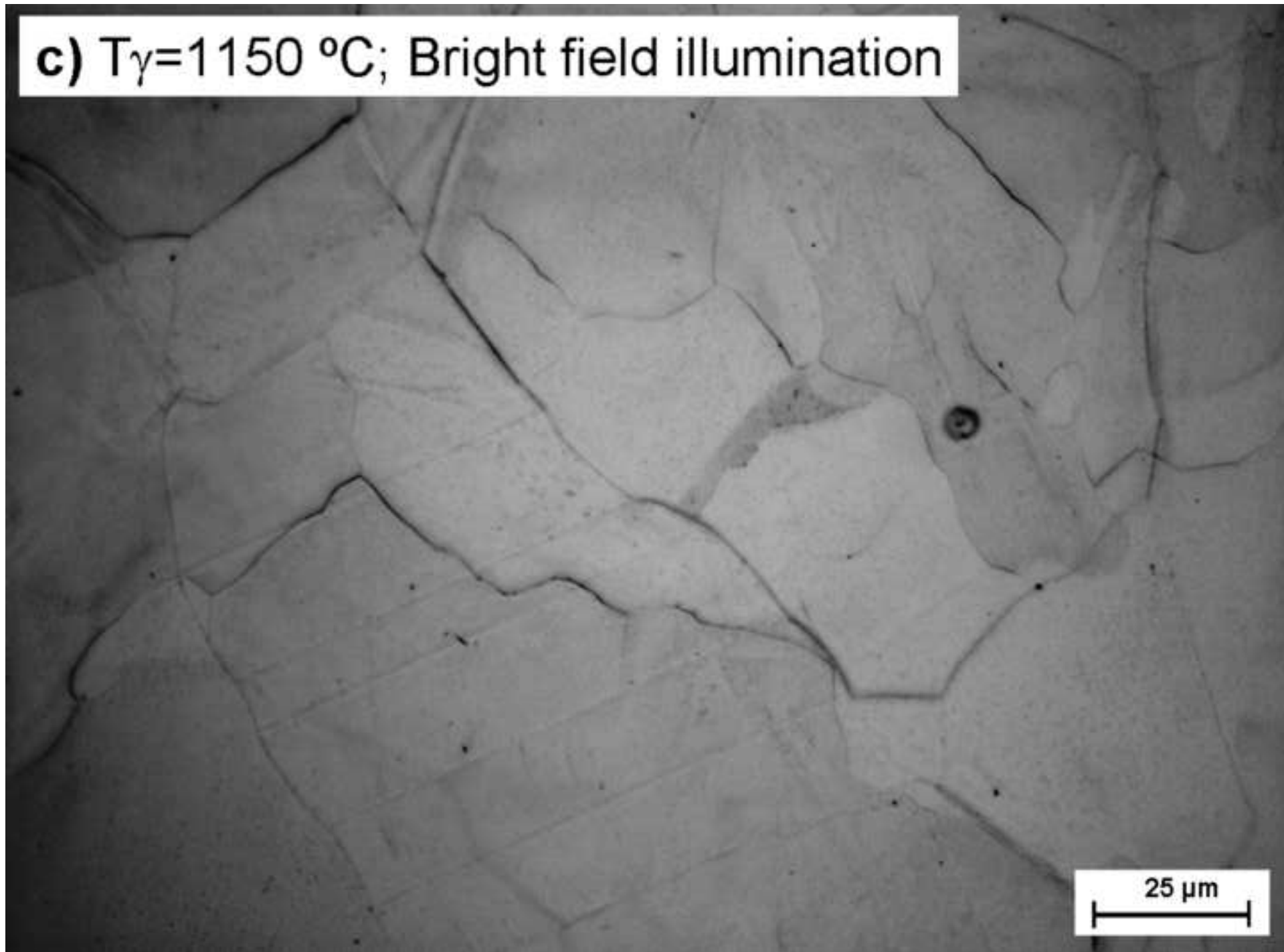


Figure 4d

**d)  $T_{\gamma}=1150$  °C; Nomarski microscopy**

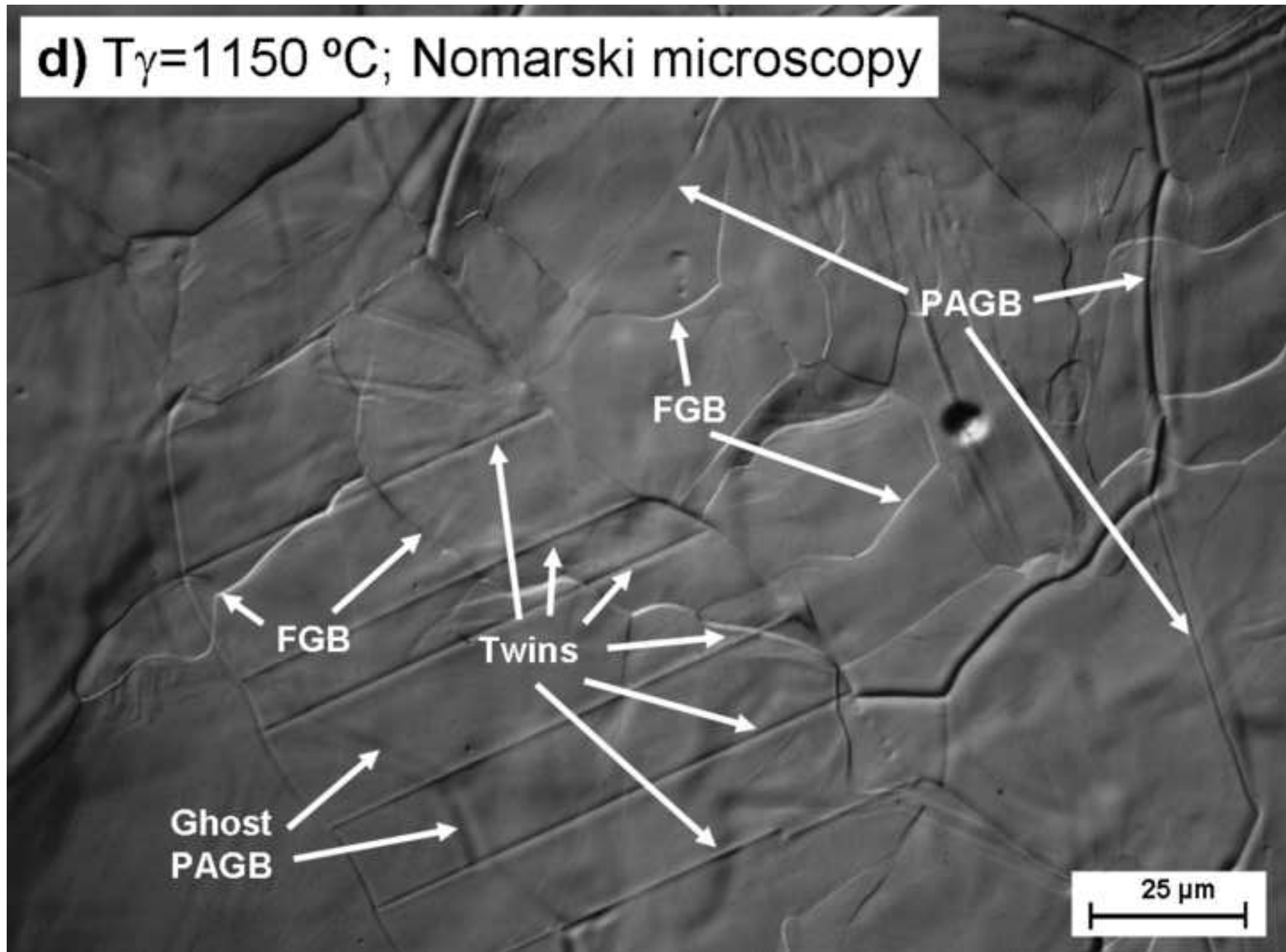
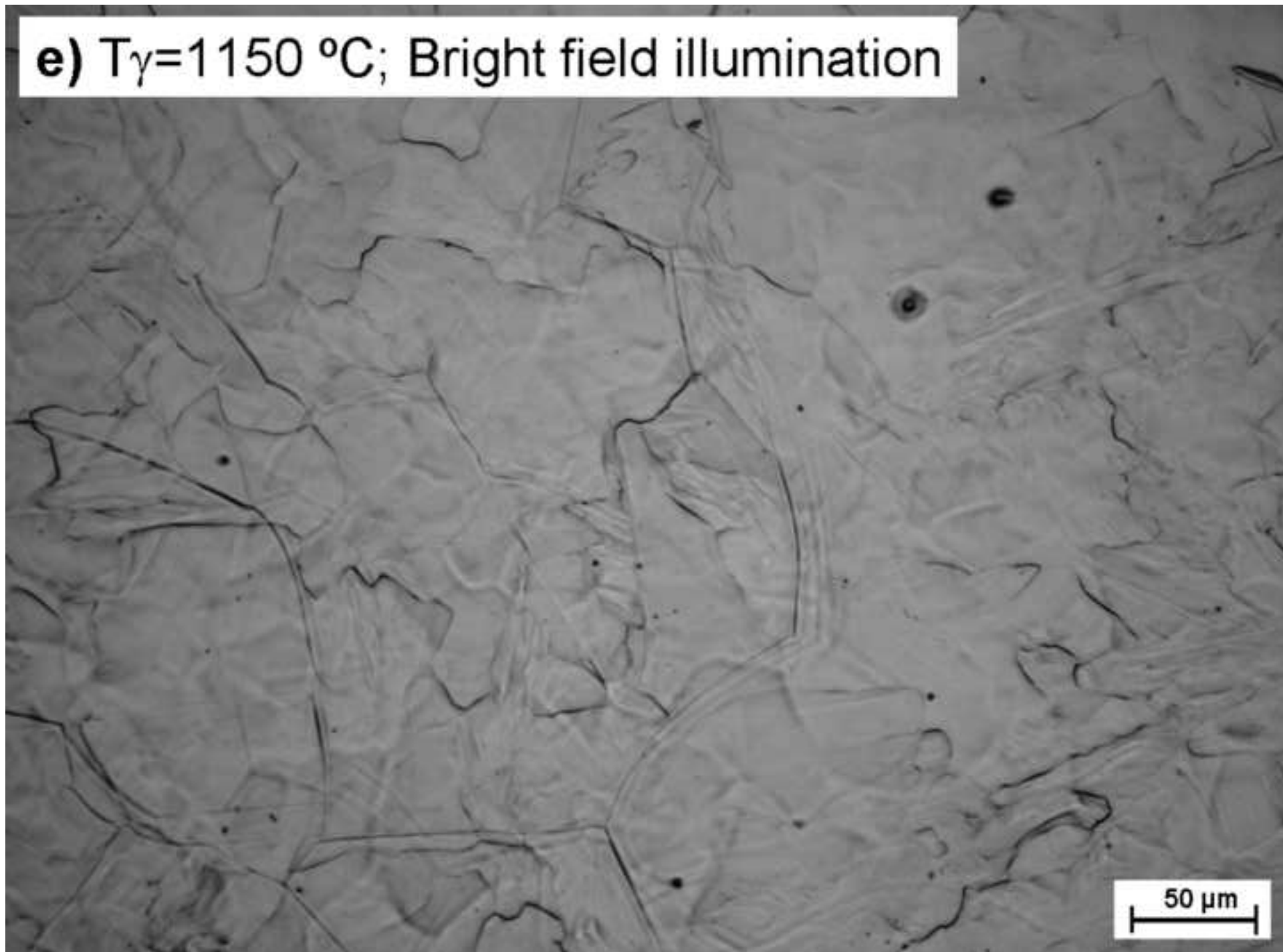


Figure 4e

**e)**  $T_{\gamma}=1150\text{ }^{\circ}\text{C}$ ; Bright field illumination





**f)**  $T_{\gamma}=1150$  °C; Nomarski microscopy

